3-2-99

NATIONAL RADIO ASTRONOMY OBSERVATORY

SUITE 219, 2015 IVY ROAD CHARLOTTESVILLE, VA 22903-1733

TELEPHONE 804-296-0334 FAX 804-296-0324

MEMO

To: John Webber

From: Skip Thacker

Date: March 2, 1999

Subject: MMA Total Power: Correlation Receivers Rev 3

Introduction

One of the requirements for the MMA is to observe with broad bandwidths in single dish total power mode. This puts some very stringent specifications on receiver gain variations that do not exist for interferometric observations. Interferometric observations inherently use a correlation type of detection which is insensitive to gain fluctuations. This memo will explore how correlation receivers can be applied to the single dish total power mode of the MMA.

The fundamental source of gain variations is the 1/f noise in the HEMT amplifiers that are used for front end and IF amplifiers. Marian W. Pospieszalski and Edward J. Wollack state in MMA Memo 222, "Obviously, the sensitivities limited by bandwidth and the system noise temperature can be attained only in a proper receiver design, as, for example, Dicke receiver with sufficiently fast switching, correlation receiver, etc." In Chapter 5 section 4 of the MMA Project Book they with John Webber quantify the problem explicitly:

> For wideband continuum observations, however, gain fluctuations will be the dominant factor. As a concrete example, consider a time scale of 1 second, which might be typical of a single unidirectional scan employed for observing a continuum point source or making a continuum map. The square of the variance in gain at 20 K ambient temperature for InP devices is about 3.6 .10-8 [1/Hz] per stage; conservatively, 6 stages of gain will be needed to obtain at least 30 dB of gain before a mixer. With 6 stages and a bandwidth of 8 GHz, a total power radiometer will have sqrt(3.6 .10-8 * 6 * 8 .109 * 0.5) = 29 times the variation in measured (delta T)/T than predicted from pure noise.

The gain variation goes [note that 30 dB at 100 GHz is 6 stages but only 3 at 18 GHz] as the number of stages and inversely to the square root of the width of the gate of the HEMT. [Project Book 5.4] One hundred GHz amplifiers typically use 50 micron gate widths while the SIS IF amplifiers can use transistor with gate widths in the order of 300 to 400 micron.

The National Radio Astronomy Observatory is a facility of the National Science Foundation operated under cooperative agreement by Associated Universities, Inc.

Galium Arsenide transistors have less 1/f noise than indium phosphide transistors so it is desirable to use GaAs transistors in the IF after a sufficient amount of gain is obtained with low noise InP transistors that the higher noise temperature of the GaAs is tolerable [reference]. The factor of 29 degradation in sensitivity is just the degradation due to the 100 GHz HEMTs in addition there is about 40 to 60 dB of IF gain as well as post detection DC gain that will add to the gain variations of the receiver.

While it is beyond the scope of this memo to discuss the effects of total power gain variations on the various science objectives of the MMA, it is the opinion of the author(s) that the receiver options described in the following sections will (may?) be necessary for meeting major science objectives. Don't single dish total power measurements grow in importance as the dish diameter is increased because of the larger minimum spacing on the compact array with the larger dishes?

An important application for correlation receiver is in the antenna evaluation receiver. John Payne in Project Book chapter 5.1 raises the issue of gain stability of the antenna evaluation receivers. In comparison to the 100 GHz receiver, the 35 GHz receiver uses 100 micron HEMTs instead of 50 micron HEMTs and 4 stages instead of 6 so its gain variation will be about half of the 100 GHz receivers IE a factor of 15 instead of 29. Which seems to me to be a problem for precise single dish measurements for this receiver as well as the 100 GHz system.

HEMT Receivers

The MMA total power mode cries out for a correlation receiver of the type shown in figure 7-21 of Kraus (see attached references). An example block diagram of how a 100 GHz correlation receiver could be constructed using HEMT amplifiers is attached as figure 1. An elementary analysis shows that (under the assumption that the gain changes are uncorrelated) the correlation receiver is insensitive to gain variation is given in the appendix. The MAP project uses NRAO 100 GHz amplifiers in a psuedo-correlation receiver for the MAP cosmic background satellite and is a clear demonstration that NRAO HEMT amplifiers and the other required components can be phase and gain matched to the degree required for a successful correlation receiver.

It is not unreasonable to expect a correlation receiver with individual gain and phase match over each 2 GHz sub band to have a factor of 100 less gain variation than the same amplifier in a single channel configuration. The cost of such improvement is that the number of RF Amplifiers and IF channels in the receiver are doubled. This scheme requires the same number of back end channels (mixer, filter, sampler, digital filter, and correlator) as the upper and lower sideband SIS system.

In the case where the correlation is done at the central building, the signals that are to be correlated must go through independent Fiber Optic Modulators and demodulators to insure that the transmission gains are uncorrelated.

SIS Receivers

One can follow a similar strategy with the SIS receivers and construct double the number of SIS mixers and IF channels to make a correlation receiver. However, it is possible to make a correlation receiver by only adding extra IF amplifiers and the associated IF channels to the balanced sideband separating mixer. The scheme shown in figure 2 generates four IF outputs from the dewar and then combines them in quadrature hybrids to obtain the four IF signals jEl, -jEl, Eu, and -Eu. By placing IF amplifiers after each of the SIS mixer elements instead after the 180 degree hybrid we have four channels that when combined in 90 degree IF hybrids give the same signals as in the correlation scheme described for the HEMT amplifier above. Forming the difference between the EL signals in an IF hybrid or digitally after the sampler gives the Lower sideband and similarly for the Upper sideband. Comparison with the conventional image separating mixers show that LO noise cancels in the upper and lower outputs in this modified scheme as well. This demonstrates that the scheme in figure 2 is equivalent to figure 5.3.5 of the project book. By adjusting the phase and amplitude of each 2 GHz band before the difference operation the LO noise canceling can be optimized. This may result in significant relaxing of the LO noise specification which is a concern at the higher bands.

The advantage is that there are now the four IF signals which can be correlated to get a total power that is insensitive to gain fluctuations. The correlation can be done either at the antenna or in the central control building as was discussed in the HEMT amplifier case. It is noted that in the SIS mixer scheme as shown in figure 2, the LO noise going into the correlators is correlated and will appear in the total power output. It is expected that this will be a constant offset that is stable with time and antenna position and could be removed with conventional position switching techniques. The stability of the LO noise now becomes a parameter that needs to be measured on the prototype LO system. Considerations of how much this LO noise contributes to the total power noise temperature will impact the specification on the allowed LO noise. This scheme requires the twice the number of IF amplifiers and back end channels (mixer, filter, sampler, digital filter, and correlator) as the conventional upper and lower sideband SIS system.

Appendix

Analysis of simple correlation receiver see figure 1.

Note the similarity figure 1 to block diagram of Predmore figure 1 (see attached references). Paralleling Predmore's analysis except substituting (G1 + deltaG1) for his G1 and G2 + deltaG2 for his G2 where my G1 is the average value of the gain and deltaG1 is a zero mean RV that is uncorrelated with any of the T's and G's in the other channel. Under this assumption and with gain and phase match between channels, this type of receiver is insensitive to gain fluctuations. The MAP project uses NRAO 100 GHz amplifiers in a psuedo-correlation receiver for the MAP cosmic background satellite and is a clear demonstration that NRAO HEMT amplifiers and the other required components can be phase and gain matched to the degree required for a successful receiver. Errors come in due to the directivity of the input and output hybrids and with gain fluctuations that are common between the two channels, for example those due common power supply voltages or temperature variations.

Let

$Ta = AA$
$Tl = BB$
$TR1 = R_1 R_1$
$TR2 = R_2 R_2$

$$Vout\_1 = (A + L + R_1) * (G1 + deltaG1)$$

$$Vout\_2 = (A - L + R_2) * (G2 + deltaG2)$$

Adjust such that G1 = G2 and absorb SqRt(kBZ_0) into the gain

$$Vout\_1 * Vout\_2 = (AA - AL + AR_2 + AL - LL + LR_2 + AR_1 - LR_1 + R_1R_2) *$$

$$(G1G2 + G1deltaG2 + G2deltaG1 + deltaG1deltaG2)$$

Now take the time average and all uncorrelated products go to zero

$$\overline{Vout\_1 * Vout\_2} = (Ta - Tl) G1G2$$

Analysis of SIS SSB (balanced mixer) see figure 2

When comparing figure 2 to project book figure 5.3.3a (Block diagram of an SIS sideband separating mixer), note that there is a different convention used for quadrature hybrids. The project book assumes the 90 phase delay is in the upper output and figure 2 assumes the 90 degree phase delay is in the lower output. After allowing for this we see that the upper and lower signal paths of figure 2 form a SSB mixer exactly like figure 5.3.3a except that the LO is delayed 90 degrees. In a similar way the middle paths form a SSB mixer except that in this case both signal paths have an additional 90 degree delay. Comparing figure 2 with 5.3.4a (Block diagram of a balanced SIS mixer) we can consider the top two signal paths of figure 2 to be a balanced mixer and LO noise in their outputs when subtracted will cancel. Ditto for the bottom two paths and the combination of the two signals at the output of the hybrids. While the LO noise cancels for the case where we difference the two outputs, the LO noise correlated and will appear in the total power output. This is true even if we use separate LO's for the upper pair and the lower pair although it will be reduced (by a factor of 1.4).

By bringing all four signals outside the dewar we can correlate to get total power or subtract for the standard processing as an interferometer element. What this scheme is really doing is using the balanced mixer part of the original design to serve double duty as an unbalanced correlation receiver and a balanced non-correlation receiver.

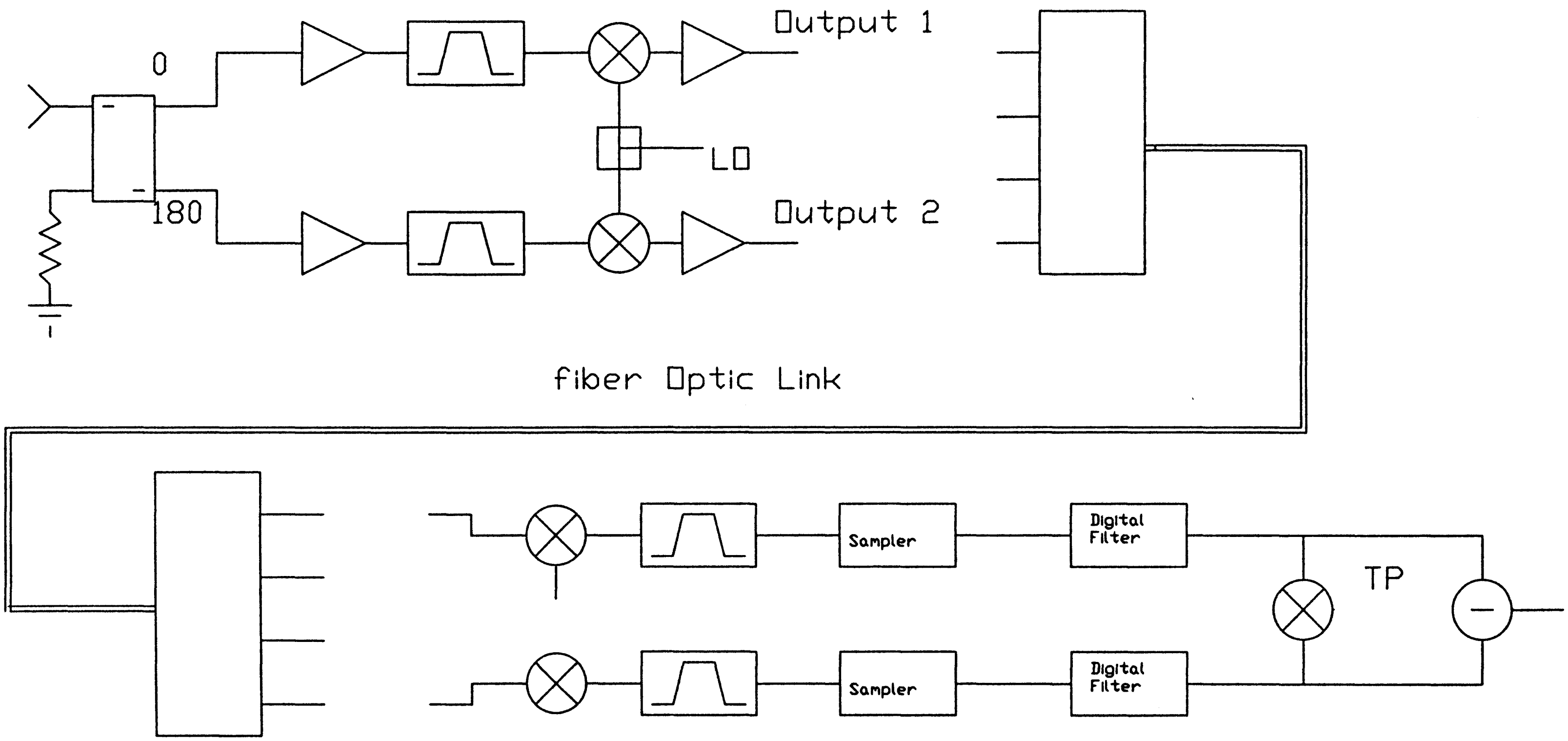

0
180
Output 1
Output 2
LO
fiber Optic Link
Sampler
Sampler
Digital Filter
Digital Filter
TP

Fig 1

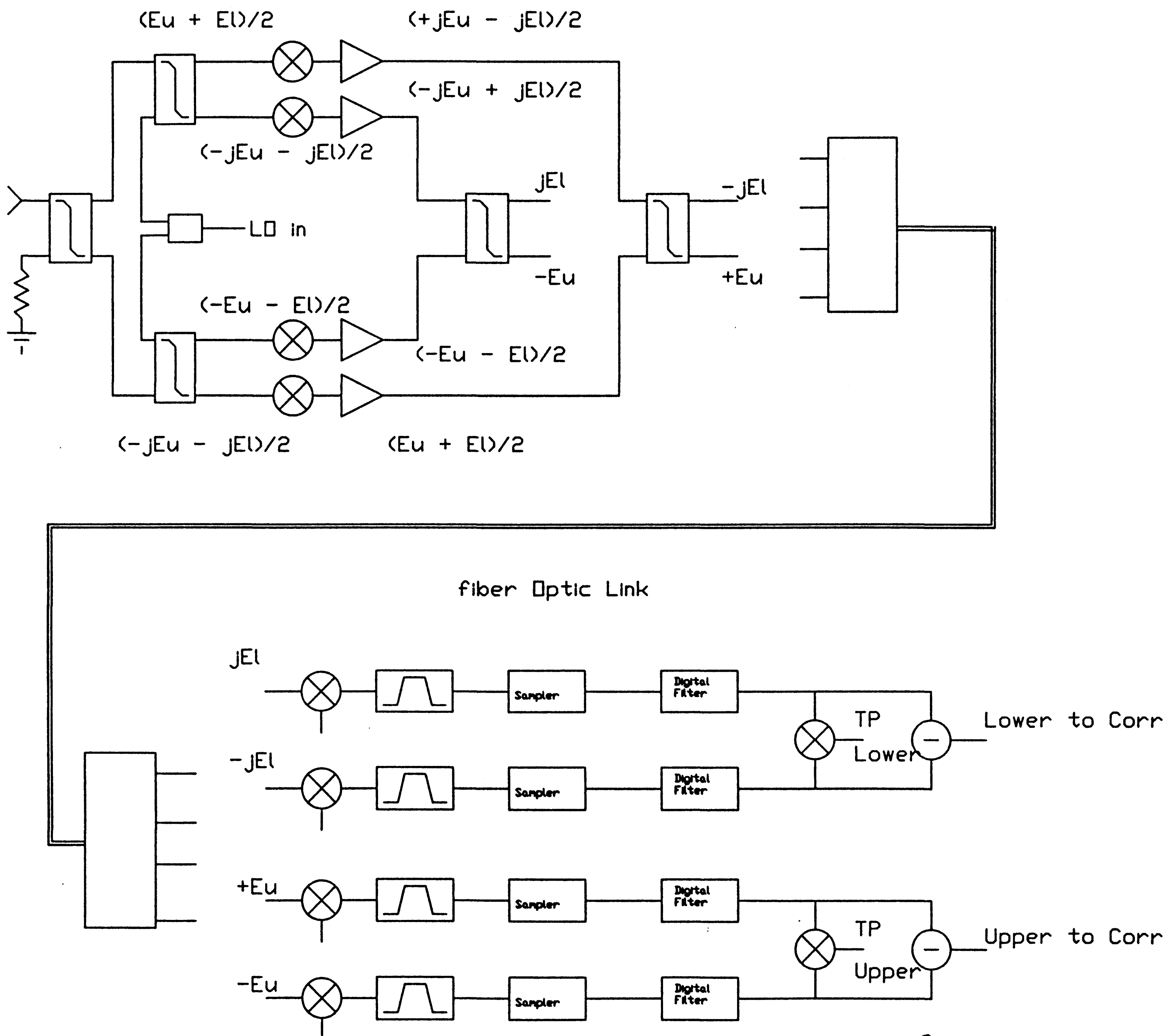
(Eu + El)/2
(+jEu - jEl)/2
(-jEu + jEl)/2
(-jEu - jEl)/2
jEl
-jEl
LO in
-Eu
+Eu
(-Eu - El)/2
(-Eu - El)/2
(-jEu - jEl)/2
(Eu + El)/2
fiber Optic Link
jEl
-jEl
+Eu
-Eu
Sampler
Digital Filter
TP
Lower
Lower to Corr
TP
Upper
Upper to Corr

Fig 2

When uncorrelated noise voltages due to the noise temperatures T_{s1} and T_{s2} are multiplied, the product has an average value zero (zero d-c output voltage from the multiplier). As in the detector of the total-power receiver the uncorrelated noise-voltage components from both receivers beat with each other in the multiplier, resulting in a low-frequency, fluctuating noise-voltage output. Referring to (7-11) for the total-power receiver, the fluctuating noise power from the integrator will be

$$W_{LF} = G_{LF}C'kT_{s1}kT_{s2}\,\Delta\nu_{HF}\,\Delta\nu_{LF} \tag{7-38}$$

A discrete source produces correlated signal-noise powers $k\,\Delta T\,\Delta\nu_{HF}$ at the receiver inputs and corresponding IF output voltages with amplitudes

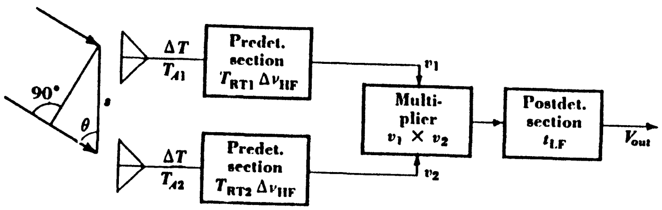

Fig. 7-19. Interferometer with correlation receiver.

proportional to $\sqrt{k\,\Delta T\,\Delta\nu_{HF}}$. If both are in phase, the multiplier output d-c voltage is proportional to $k\,\Delta T\,\Delta\nu_{HF}$. If the phase angle between them is ϕ, the d-c output voltage is equal to $k\,\Delta T\,\Delta\nu_{HF}\cos\phi$. The signal output power from the integrator is, from (7-12),

$$W = G_{LF}C'(k\,\Delta T\,\Delta\nu_{HF})^2\cos^2\phi \tag{7-39}$$

The sensitivity of the correlation receiver is obtained by putting $W = W_{LF}$ from (7-38) and (7-39), or

$$\Delta T_{\min} = \frac{1}{\cos\phi}\sqrt{\frac{T_{s1}T_{s2}\,\Delta\nu_{LF}}{\Delta\nu_{HF}}} \tag{7-40}$$

or if $T_{s1} = T_{s2} = T_{sys}$ and $t_{LF} = 1/2\Delta\nu_{LF}$

$$\Delta T_{\min} = \frac{1}{\sqrt{2}\cos\phi}\,\frac{T_{sys}}{\sqrt{\Delta\nu_{HF}\,t_{LF}}} \tag{7-41}$$

The sensitivity of a correlation receiver is hence $2\sqrt{2}$ times better than the sensitivity of a Dicke receiver with the same system noise temperature and one antenna.

Because only correlated noise voltages give a d-c output, voltage-gain instabilities will not affect the sensitivity of the correlation receiver. Gain variation will change only the calibration of the receiver. However, random phase variations in the amplifiers of the predetection sections are undesirable (Fujimoto, 1964). For the same reason scintillations in the

ionosphere will reduce the sensitivity. One of the advantages of the correlation receiver is that there is no switch and, hence, no extra losses between the antenna and the receiver, which means that the noise temperature of the receiver will be lower.

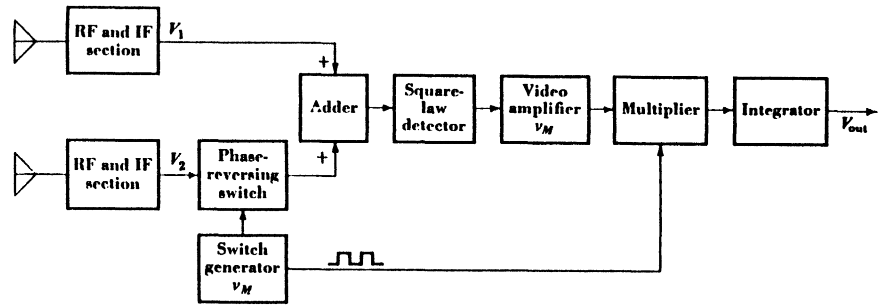

Fig. 7-20. Phase-switched receiver

The correlation principle is also applied in the phase-switched interferometer (Ryle, 1952) in Fig. 7-20. The IF signal of one receiver goes through a phase-reversing switch, which is operated at the frequency ν_M. If signals v_1 and v_2 are uncorrelated, the switching will have no effect on the square-law-detector output. When v_1 and v_2 contain correlated components, the detector output is different for $v_1 + v_2$ and for $v_1 - v_2$. This means that the detector output varies at the frequency ν_M because of the correlated

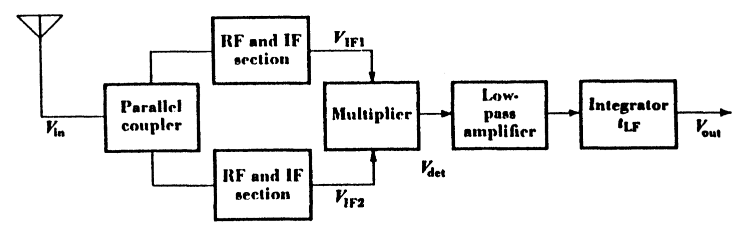

Fig. 7-21. Correlation receiver.

signal. Assuming that the desired signal is the only correlated signal, it is clear that the sensitivity of the phase-switching receiver is the same as the sensitivity of the simple Dicke receiver using a similar low-frequency section (O'Donnell, 1963).

The correlation technique can be used with one antenna by dividing the output signal from the antenna between two identical receivers (Fig. 7-21). In this case the antenna noise power ($T_A/2$) is also correlated in addition to signal noise. Hence, this modification is useful only when T_A

A Continuous Comparison Radiometer at 97 GHz

C. READ PREDMORE, MEMBER, IEEE, NEAL R. ERICKSON, G. RICHARD HUGUENIN, MEMBER, IEEE, AND PAUL F. GOLDSMITH, MEMBER, IEEE

Abstract —A continuous comparison radiometer has been implemented at 97 GHz using quasi-optical techniques for local oscillator (LO) injection and realization of a 90° hybrid. Cryogenically cooled Schottky-diode mixers and FET amplifiers give a double-sideband (DSB) system temperature of 250 K. The system is self-calibrating and optimized under computer control. The root-mean-square (rms) fluctuations due to the receiver are less than 0.025 K with a 1-s integration time.

I. Introduction

A HIGH-SENSITIVITY, continuous comparison radiometer has been implemented by the Five College Radio Astronomy Observatory. The continuous comparison or correlation radiometer circuit is over twenty years old [1] and has been used for radio astronomical observations at 74 cm [2], 11 cm [3], and 6 cm [4]. Its use at millimeter wavelengths has been precluded due to the losses and imperfections in the available waveguide components. The extensive use of quasi-optical techniques for beam guidance, local oscillator (LO) injections, and a combination of the two beams in an input hybrid has resulted in major performance gains for the system described here.

The classical problem in radiometry is to distinguish a weak source in the presence of the much greater noise from the receiver and atmosphere and in the presence of fluctuations in receiver gain and atmospheric emission. For an astronomical object such as a quasar, this is accomplished by actually moving the telescope between the source position and an adjacent position at the same elevation at a 0.05–0.10-Hz rate, deflecting the beam by nutating the subreflector at a 0.5–5-Hz rate [5], Dicke switching [6] against a load, or deflecting the beam near the Cassegrain focal plane with a rotating beam chopper at up to 50 Hz [7].

In contrast, the continuous comparison radiometer has no moving parts for switching, so that the complexities of mechanical switching systems mentioned above, and the significant loss and mismatch of a ferrite switch, are avoided. Rather, two beams are continually subtracted to give the desired difference signal with an equivalent time constant which can be short as the reciprocal of the intermediate frequency (IF) bandwidth. Since the subtraction is performed continuously, fluctuations with very short time scales that are common to both beams are cancelled perfectly. In addition, the subtraction in the radiometer is insensitive to receiver gain changes.

The present system employs a LO frequency of 97 GHz and is sensitive to input signals in both sidebands with a separation from the LO of 4.4 to 5.0 GHz. The radiometer consists of a calibration system, cryogenic front end, and IF and signal processing units. The entire system is automatically optimized, calibrated, and operated by a computer. The root-mean-square (rms) sensitivity due to the receiver is less than 0.025 K with a 1-s integration time.

II. Basic Theory

The radiometer block diagram is shown in Fig. 1. The two input beams with temperature T_A and T_B as well as the 97.3-GHz LO are split by a quasi-optical 90° hybrid and double-sideband (DSB) mixed to 4.7 GHz. At 4.7 GHz, the voltages in the two IF amplifiers are proportional to $A - jB$ and $A + jB$, where A and B are the voltages of the inputs to the Dewar. The second frequency conversion is from 4.7 to 2.1 GHz using a 6.8-GHz LO. One of the LO lines has a 6-bit computer-controlled phase shifter with a 5.6° resolution to optimize the system sensitivity. Also under computer control are 0–50-dB p-i-n attenuators in each of the 2.1-GHz IF chains. Precision IF 180° hybrid, matched detectors, and an instrumentation operational amplifier are used to multiply the two IF signals.

The resultant response of the system is

$$V_{\mathrm{DIFF}} = C_{\mathrm{DIFF}}(T_A - T_B)\cos\phi \tag{1}$$

where C_{DIFF} is a calibration constant and ϕ is the phase of the LO phase shifter. Thus, the system is insensitive to gain fluctuations and is responsive only to the input temperature difference. A manual delay line with a 0.2-ns range is used to compensate for phase slopes in the cabling and amplifiers. The entire system is automatically optimized and calibrated with a ModComp MODACS computer.

Faris [1] has done an extensive analysis of correlation radiometers including the effects of nonidentical amplifiers, gain fluctuations, and differential phase and delay. Here, the system response will be analyzed for a single IF frequency to investigate the effect of amplitude imbalance in the input 90° hybrid and imperfect balance in the final IF detectors.

Manuscript received December 19, 1983; revised August 2, 1984. This work was supported in part by the M.I.T. Lincoln Laboratory under Contract F19628-80-C-0002.

The authors are with the Five College Radio Astronomy Observatory, University of Massachusetts, Amherst, MA 01003.

Reprinted from *IEEE Trans. Microwave Theory Tech.*, vol. MTT-33, no. 1, pp. 44–51, Jan. 1985.

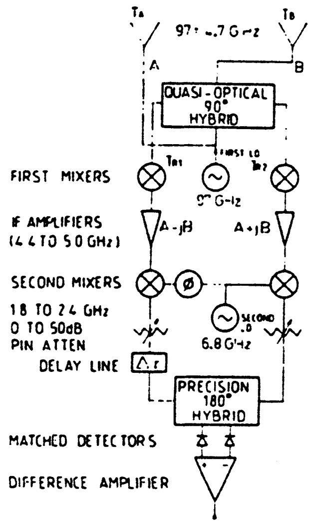

Fig. 1. Radiometer block diagram. The two inputs at temperatures of T_A and T_B are split and combined in a quasi-optical hybrid. After mixing at 97 GHz, they are amplified and phase shifted to optimize the response. A precision 180° hybrid and matched detectors are used to "multiply" the two IF signals.

The amplitude of the incoming signal in the upper sideband (USB) and in the lower sideband (LSB) is proportional to the square root of the input temperature. In the following equations, the unprimed quantities are from the USB and primed quantities from the LSB. The complex conjugate is represented by the symbol (*). The input temperatures in the signal and reference beams are denoted by T_A and T_B, respectively, and the two receiver temperatures are T_{R1} and T_{R2}. The signal amplitudes are A and A' and the reference amplitudes B and B', in the two sidebands. The amplitudes for the receiver noise in channels 1 and 2 are R_1 and R'_1 and R_2 and R'_2, respectively. These amplitudes are related to the temperatures by

$$T_A = A \times A^* + (A') \times (A')^* \tag{2a}$$

$$T_B = B \times B^* + (B') \times (B')^* \tag{2b}$$

$$T_{R1} = R_1 \times R^*_1 + (R'_1) \times (R'_1)^* \tag{2c}$$

$$T_{R2} = R_2 \times R^*_2 + (R'_2) \times (R'_2)^*. \tag{2d}$$

In general, the 90° beam-splitter hybrid does not split the signals equally but has amplitudes of ρ for reflection and τ for transmission, which are assumed to be the same for both sidebands. Depending on how the LO is injected, the continuous comparison radiometer can be realized with a 180 or 90° input hybrid. After going through the quasi-optical hybrid, the signal amplitudes are

$$V_1 = j\exp(j\omega_{\mathrm{LO}}t)\{1 + (\rho A - j\tau B + R_1)\exp(j\omega_1 t) + (\rho A' - j\tau B' + R'_1)\exp(-j\omega_1 t)\} \tag{3a}$$

$$V_2 = \exp(j\omega_{\mathrm{LO}}t)\{1 + (\tau A + j\rho B + R_2)\exp(j\omega_1 t) + (\tau A' + j\rho B' + R'_2)\exp(-j\omega_1 t)\} \tag{3b}$$

where j is the square root of (-1), ω_{LO} the angular frequency of the 97-GHz LO, ω_1 the first IF angular frequency, and t is time. The signal level of the 97-GHz LO is represented by the first term in the expressions for V_1 and V_2. It is arbitrarily set to 1 to show the phase of the LO. The second and third terms are the upper and lower sidebands, respectively.

After double-sideband mixing with the 97-GHz LO, gain at the first IF and LSB mixing from 4.7 (ω_1) to 2.1 GHz (ω_2) with a 6.8-GHz second LO, the voltages are

$$V_3 = \exp(j\phi)G_1\{(\rho A - j\tau B + R_1)\exp(-j\omega_2 t) + (\rho A' - j\tau B' + R'_1)\exp(j\omega_2 t)\} \tag{4a}$$

$$V_4 = G_2\{(\tau A + j\rho B + R_2)\exp(-j\omega_2 t) + (\tau A' + j\rho B' + R'_2)\exp(j\omega_2 t)\} \tag{4b}$$

where the term $\exp(j\phi)$ is the relative phase shift introduced by the 6.8-GHz phase shifter and G_1 and G_2 are the voltage gains in the two channels.

At the output of the precision 180° IF hybrid, the voltages are

$$V_5 = (V_3 + V_4)/\sqrt{2} \tag{5a}$$

$$V_6 = (V_3 - V_4)/\sqrt{2}. \tag{5b}$$

The detected power is obtained by multiplying V_5 and V_6 by their complex conjugates and low-pass filtering to remove harmonics of the IF components. Cross products such as $A \times B$ and $R_1 \times R_2$ will average out to zero when the inputs are uncorrelated and there is no correlated noise in the two receiver temperatures. In the following discussion, K and $K(1-\delta)$ represent the product of the detector sensitivities and difference amplifier gains for the two detected outputs, where the magnitude of (δ) is less than 0.05. In this case, the voltage, of the two outputs are

$$\begin{aligned} V_7 = [K/2]\{&T_A[(\rho G_1)^2 + (\tau G_2)^2 + (2\rho\tau G_1 G_2)\cos(\phi)] \\ &+ T_B[(\tau G_1)^2 + (\rho G_2)^2 - (2\rho\tau G_1 G_2)\cos(\phi)] \\ &+ T_{R1}(G_1)^2 + T_{R2}(G_2)^2 \end{aligned} \tag{6a}$$

$$\begin{aligned} V_8 = {}&[K(1-\delta)/2] \\ &\cdot\{T_A[(\rho G_1)^2 + (\tau G_2)^2 - (2\rho\tau G_1 G_2)\cos(\phi)] \\ &+ T_B[(\tau G_1)^2 + (\rho G_2)^2 + (2\rho\tau G_1 G_2)\cos(\phi)] \\ &+ T_{R1}(G_1)^2 + T_{R2}(G_2)^2\}. \end{aligned} \tag{6b}$$

Then, the output of the radiometer is the difference of V_7 and V_8

$$\begin{aligned} V_{\mathrm{out}} = K\{&[(2\rho\tau G_1 G_2)(T_A - T_B)\cos(\phi)] \\ &+ (\delta/2)\{T_A[(\rho G_1)^2 + (\tau G_2)^2] \\ &+ T_B[(\tau G_1)^2 + (\rho G_2)^2)] \\ &+ T_{R1}(G_1)^2 + T_{R2}(G_2)^2\}. \end{aligned} \tag{7}$$

The quartz beam splitter splits the signal with 54 percent of the incident power being reflected and 46 percent transmitted. This gives values for ρ and τ of 0.750 and 0.667, so that $(2\rho\tau)$ equals 0.996. When the two IF gains are equal, as is the case for normal operation, the system output is proportional to the input temperature difference plus a fractional offset term due to the detector imbalance. In this case, the output is given by

$$V_{out} = (KG_1G_2)\{(T_A - T_B)\cos(\phi) + (\delta)[(T_A + T_B)/2 + (T_{R1} + T_{R2})/2]\}. \quad (8)$$

With the precision IF hybrid and careful matching of the detectors, δ can be reduced to less than 0.001. This will give an offset on the order of 0.5 K, which can be measured by cycling through the second LO phase ϕ, or can be subtracted out by observing the source alternately in beam A and beam B.

III. Front-End System

The two input beams are 51 mm apart at the Cassegrain focus of a 13.7-m-diam telescope with a f/d ratio of 4.0. This gives two 1.0′-diam beams which are 3.3′apart in azimuth on the sky. This close beam separation was chosen to optimize the cancellation of atmospheric effects. A wider beam separation could be designed if broader sources were to be mapped. The inputs are linearly polarized with the two polarizations 110° apart.

As is schematically shown in Fig. 2, the front-end portion of the system consists of the input optics, the scalar feeds, the cryogenic millimeter mixers, and the IF amplifiers. All of these are integrated into the cryogenics Dewar which is 250×300×400 mm in size. The top and bottom covers have O-ring and RF shielding grooves. This design has given a very reliable system. The cooling to 15 and 77 K is done with a CTI 350CP closed-cycle helium refrigerator. A 0.8-mm-thick aluminum shield is attached to the 77 K station of the refrigerator to minimize the thermal radiation loading on the 15 K components. Part of this heat shield is lined with a microwave absorber to act as a black body at 77 K for the LO signal which is not coupled into the mixers and to terminate any reflections and spillover in the optics at 77 K.

As is described in detail in the next section, the optics take the beams at the Cassegrain focus of the antenna, expand them so that the LO can be injected, and combine the two beams in the quasi-optical 90° hybrid. The beams are then refocused to match into the scalar feeds.

The 97.3-GHz LO is provided by a Gunn-diode oscillator having 10 mW of power. The output of the oscillator is isolated and attenuated before going through a waveguide vacuum feedthrough. Inside the Dewar, the LO is coupled into the optics with a rectangular horn, a rexolite focusing lens, and two flat mirrors.

Double-sideband mixing is done in a pair of Schottky-diode millimeter mixers which are cooled to 15 K. The mixers have been developed at the FCRAO and have broad-band RF filters and noncontacting backshorts. They utilize GaAs diodes which have a low doping of 3×10^{16} cm^{-3} to give an optimum performance when cryogenically cooled [8], [9]. The mixer blocks are machined from OFHC copper to minimize their RF losses and have a linear taper from full- to 1/4-height waveguide. The RF filter has been designed to present a short to the diode at 97 GHz and is reactive at the second harmonic of the LO to minimize

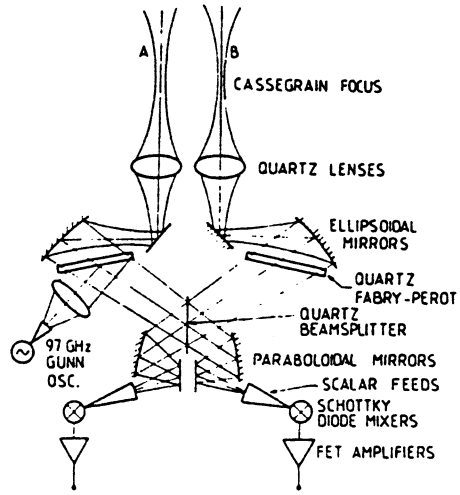

Fig. 2. Radiometer optics diagram. The symmetrical system uses fused-silica lenses to focus the inputs from the Cassegrain focus into the cryogenic Dewar. A thin sheet of fused-silica acts as a 90° hybrid. Then the 97-GHz LO is injected via a dielectric Fabry-Perot and the beams are refocused into the millimeter mixers.

conversion to higher harmonics. The noncontacting backshort has also been especially designed [10] to be a short circuit at 97 GHz and a pure reactance at 194 GHz. The backshort position was optimized at room temperature and locked into place with a setscrew before cooling the system to 15 K. The whisker length has been optimized since its length tunes the mixer response versus the input frequency [8].

Cooled circulators and FET amplifiers give an IF noise temperature of 25–30 K over the 4.4–5.0-GHz band. Each IF chain consists of an input isolator [12], FET amplifier [13], and output isolator at 20 K, providing a net gain of 11 dB. A second FET with 12 dB more gain is mounted on the 77 K station of the closed-cycle helium refrigerator. The circulators and amplifiers which were made at the FCRAO are followed by commercial amplifiers at 300 K, which are mounted within the vacuum chamber. Their 55 dB of gain gives a net RF to IF gain of 80 dB before the signals leave the RF-shielded Dewar. These signals are then processed as discussed in Section V.

IV. Optics

The input optics to the radiometer serve multiple purposes. They

1) illuminate the subreflector of the 14-m-diam telescope with a 12-dB edge taper,
2) inject the local oscillator power at 97.3 GHz,
3) combine the input beams in such a way as to create a quasi-optical 90° hybrid for the two sidebands at 93 and 102 GHz.

The optics block diagram is shown in Fig. 2. The photograph in Fig. 3 shows the front end with the vacuum Dewar removed. This view shows the optics after the fused-silica lenses. Fig. 4 shows the beam propagation in one plane so that the various optical elements and the Gaussian beam can be accurately displayed. In the actual

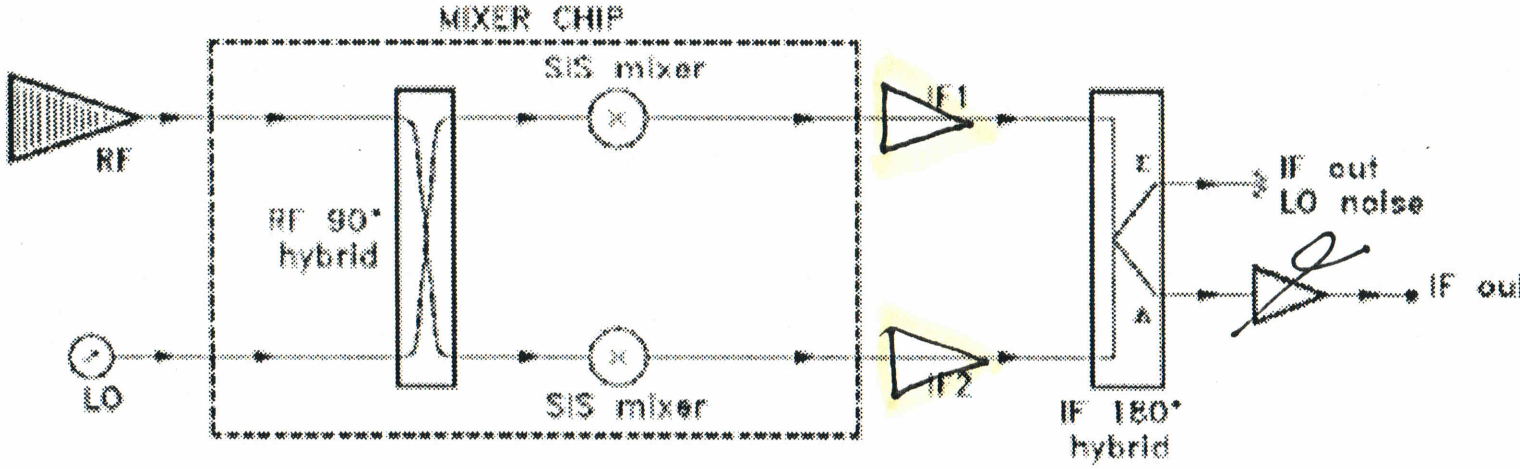

Click to zoom

Figure 5.3.4(a). Block diagram of a balanced SIS mixer.

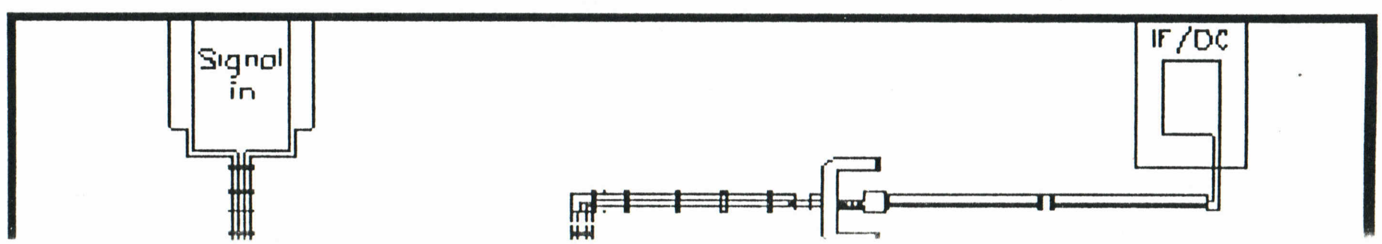

noise ıe .wanted sideband. The schematic is shov F ure 5.3.5. We expect that the mixer chip will be about 2 X 2 mm in size for 200-300 GHz.

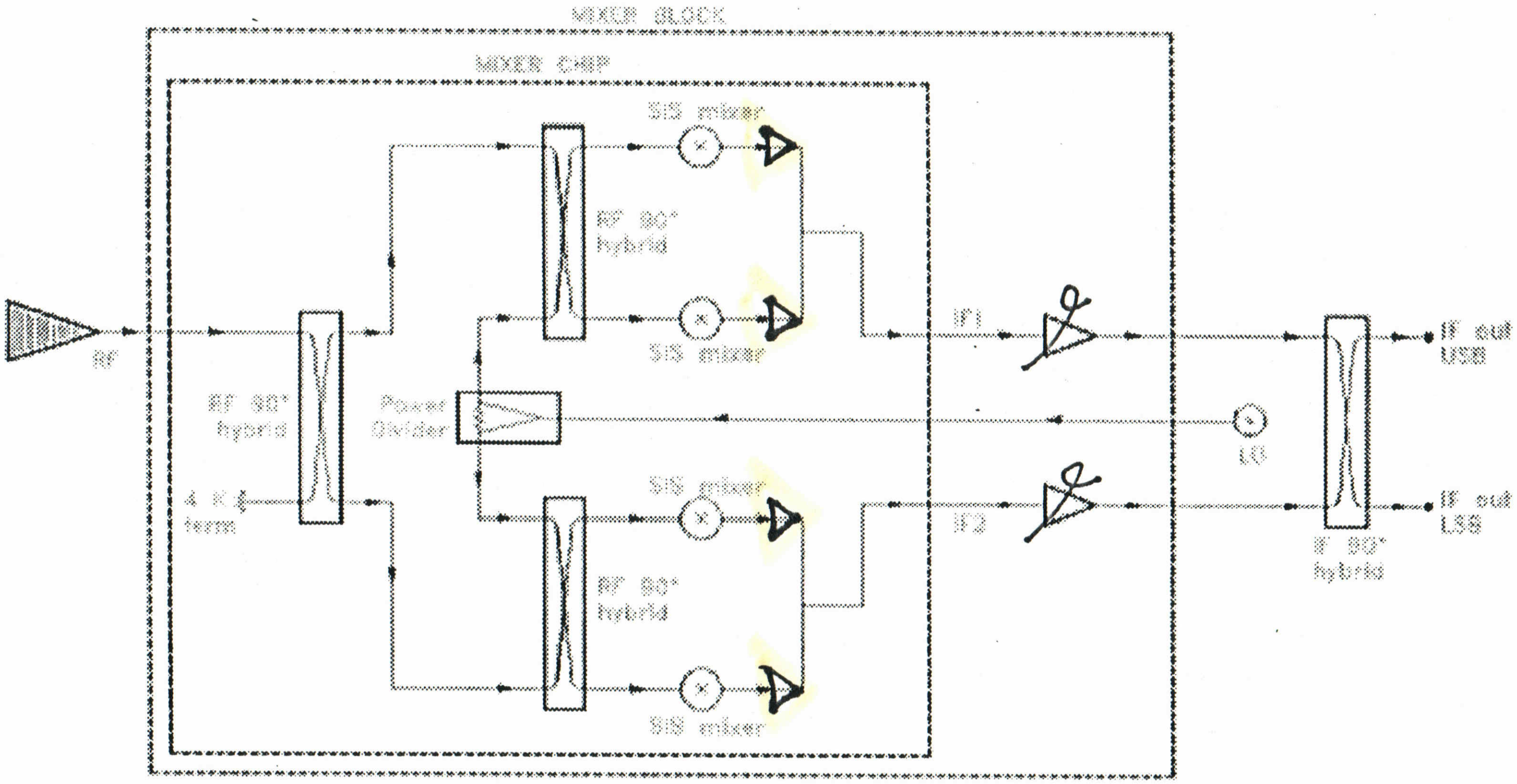

Click to zoom

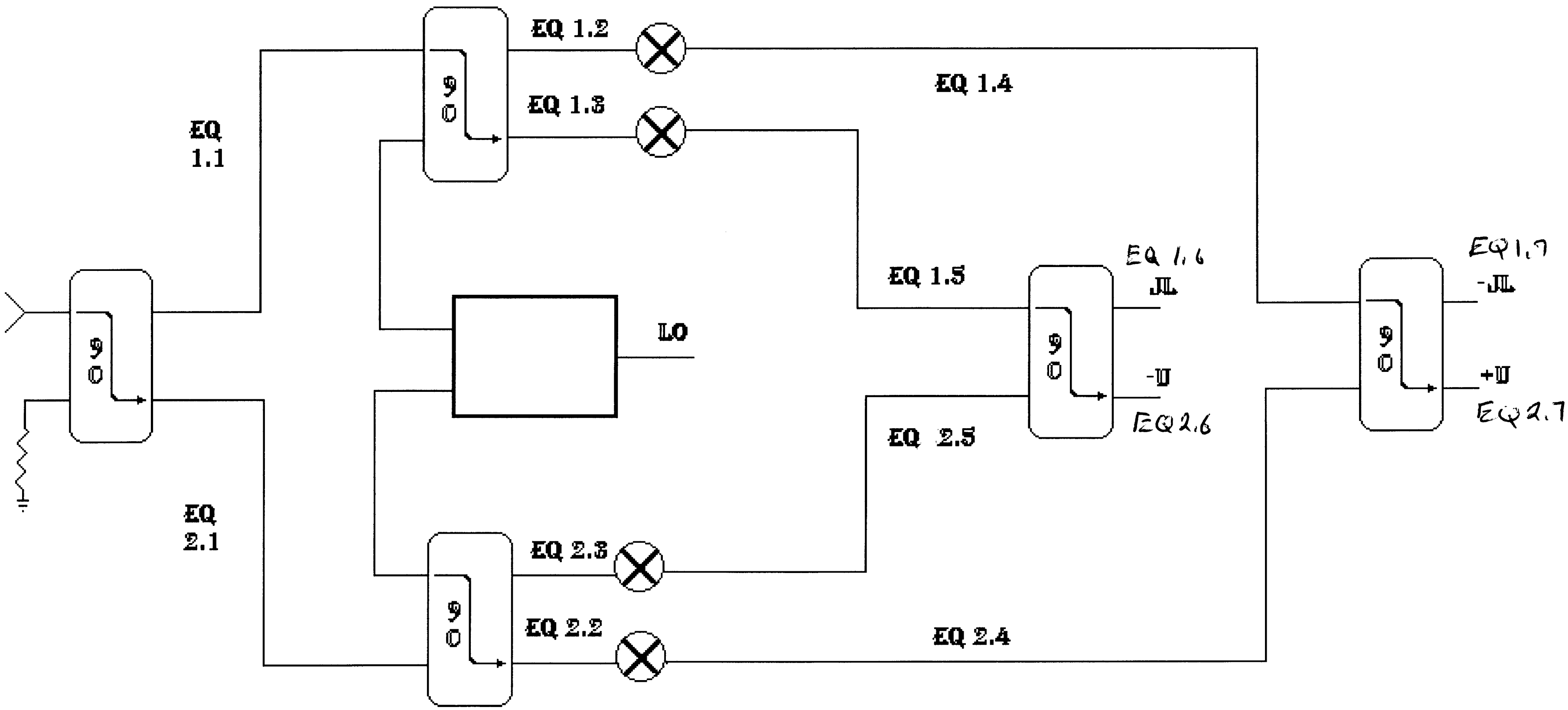
EQ 1.1
EQ 1.2
EQ 1.3
EQ 1.4
EQ 1.5
EQ 1.6
JL
-U
EQ 2.6
EQ 1.7
-JL
+U
EQ 2.7
9 0
LO
EQ 2.1
EQ 2.2
EQ 2.3
EQ 2.4
EQ 2.5

3-2-99

At the antenna input

$$E_l \cdot \cos(\omega_l \cdot t) + E_u \cdot \cos(\omega_u \cdot t)$$

Equation 1.1

$$\frac{E_l}{\sqrt{2}} \cdot \cos(\omega_l \cdot t) + \frac{E_u}{\sqrt{2}} \cdot \cos(\omega_u \cdot t)$$

Equation 2.1

$$\frac{E_l}{\sqrt{2}} \cdot \cos\left(\omega_l \cdot t - \frac{\pi}{2}\right) + \frac{E_u}{\sqrt{2}} \cdot \cos\left(\omega_u \cdot t - \frac{\pi}{2}\right)$$

Equation 1.2

$$\frac{E_l}{2} \cdot \cos(\omega_l \cdot t) + \frac{E_u}{2} \cdot \cos(\omega_u \cdot t)$$

Equation 1.3

$$\frac{E_l}{2} \cdot \cos\left(\omega_l \cdot t - \frac{\pi}{2}\right) + \frac{E_u}{2} \cdot \cos\left(\omega_u \cdot t - \frac{\pi}{2}\right)$$

Equation 2.3

$$\frac{E_l}{2} \cdot \cos(\omega_l \cdot t - \pi) + \frac{E_u}{2} \cdot \cos(\omega_u \cdot t - \pi)$$

Equation 2.2

$$\frac{E_l}{2} \cdot \cos\left(\omega_l \cdot t - \frac{\pi}{2}\right) + \frac{E_u}{2} \cdot \cos\left(\omega_u \cdot t - \frac{\pi}{2}\right)$$

In the mixing process, the phase of the IF signal due to an uppersideband signal is

$$\Phi_{\text{if\_due\_to\_upper}} = \Phi_{\text{upper}} - \Phi_{\text{lo}}$$

and the phase of the IF signal due to a lower sideband signal is

$$\Phi_{\text{if\_due\_to\_lower}} = \Phi_{\text{lo}} - \Phi_{\text{lower}}$$

Equation 1.4

$$\frac{E_l}{2}\cdot\cos\left(\omega_{if}\cdot t - \frac{\pi}{2}\right) + \frac{E_u}{2}\cdot\cos\left(\omega_{if}\cdot t + \frac{\pi}{2}\right)$$

Equation 1.5

$$\frac{E_l}{2}\cdot\cos\left(\omega_{if}\cdot t + \frac{\pi}{2}\right) + \frac{E_u}{2}\cdot\cos\left(\omega_{if}\cdot t - \frac{\pi}{2}\right)$$

Equation 2.5

$$\frac{E_l}{2}\cdot\cos\left(\omega_{if}\cdot t + \pi\right) + \frac{E_u}{2}\cdot\cos\left(\omega_{if}\cdot t - \pi\right)$$

Equation 2.4

$$\frac{E_l}{2}\cdot\cos\left(\omega_{if}\cdot t\right) + \frac{E_u}{2}\cdot\cos\left(\omega_{if}\cdot t\right)$$

Equation 1.6

$$\frac{E_l}{2\cdot\sqrt{2}}\cdot\cos\left(\omega_{if}\cdot t + \frac{\pi}{2}\right) + \frac{E_u}{2\cdot\sqrt{2}}\cdot\cos\left(\omega_{if}\cdot t - \frac{3\cdot\pi}{2}\right) + \left(\frac{E_l}{2\cdot\sqrt{2}}\cdot\cos\left(\omega_{if}\cdot t + \frac{\pi}{2}\right) + \frac{E_u}{2\cdot\sqrt{2}}\cdot\cos\left(\omega_{if}\cdot t - \frac{\pi}{2}\right)\right)$$

Simplifying

$$\frac{-1}{2}\cdot E_l\cdot\sqrt{2}\cdot\sin\left(\omega_{if}\cdot t\right)$$

or

$$\frac{E_l}{\sqrt{2}}\cdot\cos\left(\omega_{if}\cdot t + \frac{\pi}{2}\right)$$

Equation 2.6

$$\frac{E_l}{2\cdot\sqrt{2}}\cdot\cos\left(\omega_{if}\cdot t\right)+\frac{E_u}{2\cdot\sqrt{2}}\cdot\cos\left(\omega_{if}\cdot t-\pi\right)+\left(\frac{E_l}{2\cdot\sqrt{2}}\cdot\cos\left(\omega_{if}\cdot t+\pi\right)+\frac{E_u}{2\cdot\sqrt{2}}\cdot\cos\left(\omega_{if}\cdot t-\pi\right)\right)$$

Simplifying

$$\frac{-1}{2}\cdot E_u\cdot\sqrt{2}\cdot\cos\left(\omega_{if}\cdot t\right)$$

or

$$-\frac{E_u}{\sqrt{2}}\cdot\cos\left(\omega_{if}\cdot t\right)$$

Equation 1.7

$$\frac{E_l}{2\cdot\sqrt{2}}\cdot\cos\left(\omega_{if}\cdot t-\frac{\pi}{2}\right)+\frac{E_u}{2\cdot\sqrt{2}}\cdot\cos\left(\omega_{if}\cdot t+\frac{\pi}{2}\right)+\left(\frac{E_l}{2\cdot\sqrt{2}}\cdot\cos\left(\omega_{if}\cdot t-\frac{\pi}{2}\right)+\frac{E_u}{2\cdot\sqrt{2}}\cdot\cos\left(\omega_{if}\cdot t-\frac{\pi}{2}\right)\right)$$

Simplifying

$$\frac{1}{2}\cdot E_l\cdot\sqrt{2}\cdot\sin\left(\omega_{if}\cdot t\right)$$

or

$$\frac{E_l}{\sqrt{2}}\cdot\cos\left(\omega_{if}-\frac{\pi}{2}\right)$$

Equation 2.7

$$\frac{E_l}{2\cdot\sqrt{2}}\cdot\cos\left(\omega_{if}\cdot t\right)+\frac{E_u}{2\cdot\sqrt{2}}\cdot\cos\left(\omega_{if}\cdot t\right)+\left(\frac{E_l}{2\cdot\sqrt{2}}\cdot\cos\left(\omega_{if}\cdot t-\pi\right)+\frac{E_u}{2\cdot\sqrt{2}}\cdot\cos\left(\omega_{if}\cdot t\right)\right)$$

Simplifying

$$\frac{E_u}{\sqrt{2}}\cdot\cos\left(\omega_{if}\cdot t\right)$$